Simulation of density measurement in plasma wakefield using photon acceleration

Muhammad Firmansyah Kasim,[1] Naren Ratan,[1] Luke Ceurvorst,[1] James Sadler,[1] Philip Burrows,[1] Raoul Trines,[2] James Holloway,[3] Matthew Wing,[3] and Peter Norreys[1,2]

[1] *Clarendon Laboratory, Department of Physics, University of Oxford, Parks Road, Oxford, OX1 3PU, United Kingdom*
[2] *STFC Rutherford Appleton Laboratory, Chilton, Didcot, OX11 0QX, United Kingdom*
[3] *Department of Physics and Astronomy, University College London, Gower Street, London, WC1E 6BT, United Kingdom*

(Dated: May 30, 2014)

One obstacle in plasma accelerator development is the limitation of techniques to diagnose and to measure plasma wakefield parameters. In this paper, we present a density measurement of a wakefield using photon acceleration. A measurement is performed by sending a long laser pulse to move along with a wakefield. The technique can measure the perturbed electron density in the laser's reference frame, averaged over the propagation distance. From simulation, we expect a measurement to be accurate to within 10% for some propagation distance. We discuss the limitations and effects that would affect the measurement: a small frequency change, photon trapping, and laser displacement effect. By considering these effects, we can determine the optimal frequency of the laser pulse and its propagation distance for a given set of experimental parameters.

I. INTRODUCTION

Plasma acceleration has been receiving interest recently since it can accelerate electrons up to GeV energy with a length much shorter than conventional accelerators [1–4]. In a plasma accelerator, a driver beam disturbs the plasma and generates wakefields. The driver can be a short laser pulse [5], beat wave [6], electron beam [7], or proton beam [8].

Longitudinal electric fields generated in the plasma can reach up to tens or hundreds of GeV/m [9–11]. However, there is still no adequate technique to measure and diagnose the perturbed density in the plasma. One of the earliest methods to diagnose the plasma wave is frequency domain interferometry (FDI) [12]. FDI uses two short laser pulses and measures their phase difference caused by a different refractive index and density of plasma at certain positions. By using the FDI technique, we can only determine the density of plasma at certain single points. Therefore, to make a density profile, it needs painstakingly many shots of short probe pulses at different positions.

The more sophisticated technique is using frequency domain holography (FDH) [12, 13]. The FDH technique needs one short reference pulse and one long probe pulse for measurement. However, in order to diagnose plasma wakefield with order of μm, one needs a very short reference pulse with order of fs, which is much less than the wakefield wavelength. The other FDH technique is by using two long chirped pulses [14, 15]. By providing quite a wide frequency span of the chirped pulse, this technique could give more accurate results than the previous one that uses one short and one long pulse.

Another plasma imaging technique is using shadowgraph technique [16]. With this technique, the second derivation of the density with respect to the position is obtained. However, it is hard to extract quantitative data from the result of this technique because it needs small density perturbation to get the precise data.

One promising technique to measure the density profile of plasma wakefield is using photon acceleration [17–19]. In photon acceleration, we send long probe pulse to move along with the plasma wave and measure the change in frequency of the pulse. The frequency change of the pulse is caused by the slope of the plasma density profile. From the information, we can extract the density profile from the probe's frequency.

In this paper, we present the simulation results of measurement using photon acceleration in plasma wakefield. The measurement results are then compared with actual simulated value to see the accuracy of the measurement.

II. PHOTON ACCELERATION

When a photon moves in a medium which has a refractive index varying with time, the photon will undergo a change in frequency. Plasma wakefields generated in plasma accelerators propagate along the plasma and have a different refractive index in every position. Thus, if a laser propagates together with the wakefield, the laser frequency will change after some propagation distance.

Using photon ray theory by Mendonça [20], we can obtain the frequency change of a laser co-propagating with plasma wakefield as:

$$\frac{\Delta\omega}{\omega_0} \approx -\frac{\omega_p^2}{2\omega_0^2}\frac{1}{n_0}\int \frac{\partial n}{\partial \zeta}\,\mathrm{d}s, \tag{1}$$

where $\Delta\omega$ denotes the frequency change of the laser, ω_0 the central frequency of the laser, n and n_0, respectively, the perturbed and initial plasma density, $\omega_p \approx k_p c$ the plasma frequency, s the propagation distance of the laser, and $\zeta = z - ct$ denotes the position relative to the laser's frame of reference. This expression is also discussed by Dias *et al.* [17].

In order to get the density profile, we need a long laser pulse that covers several plasma wavelengths. By doing so, we can obtain the average density over the propagation distance for every position in the laser's frame of reference.

In a real experiment, it is possible to measure the frequency change of a laser in every position using frequency resolved optical gating (FROG) equipment. Schreiber *et al.* [21] have used the second harmonic generation (SHG) FROG to get the complete temporal characterisation of a laser pulse: amplitude and phase.

III. METHODS

A. Simulation parameters

Simulations were performed using OSIRIS 1D relativistic code [22] on the SCARF-LEXICON machine at STFC Rutherford Appleton Laboratory. OSIRIS uses particle in cell (PIC) [23] algorithm to solve differential equations to determine electromagnetic fields and the phase space of particles. Particles in PIC codes are modelled in super-particles model. A super-particle is a computational particle which represents many real particles. Electromagnetic fields in PIC codes are determined from the positions and momenta of the particles and thus will act on the particles changing their positions and momenta.

In this paper, we present a case for the use of a diagnostic based on photon acceleration. In the baseline set up, we send a short pump pulse with wavelength of 800 nm and with duration of 39 fs to a plasma with density of 2×10^{18} cm^{-3}. The intensity of the pump pulse is 2.1×10^{18} W/cm^2, which gives a normalised potential of $a_0 = 1.0$, to drive non-linear wakefield. In the plasma, the pump pulse generates a plasma wakefield which will be diagnosed using a probe pulse. The probe pulse is sent behind the pump pulse with the same wavelength but with a longer duration, 300 fs. The intensity of the probe pulse is much lower than the pump pulse, 2.1×10^{16} W/cm^2, which corresponds to $a_0 = 0.1$. We make the intensity of the probe pulse as small as possible so that it does not disturb the wakefield generated by the pump pulse. These pulses propagates through the plasma for distance about 7 mm.

B. Getting the local frequency

The simulation produces the actual density profile and the transverse electric field of the pump and probe pulse. We apply a transformation to the probe pulse's electric field to get its Wigner distribution [24] to represent the wave energy distribution in phase space or in time-frequency space. The Wigner distribution of a signal is represented by:

$$W_E(\zeta, k) = \int_{-\infty}^{\infty} E(\zeta+\zeta'/2)E^*(\zeta-\zeta'/2)e^{-2\pi ik\zeta'}\mathrm{d}\zeta' \quad (2)$$

where $E(\zeta)$ is electric field of the signal at position ζ relative to the laser's frame of reference and $k = 2\pi f/c$ is wavenumber of the laser. Because there are two terms of the signal multiplied together, there are cross-terms in the distribution [25].

By taking the average and weighted average of the Wigner distribution, we can get local intensity and local frequency of the probe pulse, as shown in the equations below,

$$\begin{aligned} |E(\zeta)|^2 &= \int_{-\infty}^{\infty} W_E(\zeta, k)\mathrm{d}k \\ f(\zeta) &= \frac{c}{2\pi}\frac{1}{|E(\zeta)|^2}\int_{-\infty}^{\infty} kW_E(\zeta, k)\mathrm{d}k. \end{aligned} \quad (3)$$

The denominator in the second equation indicates that we can make a good measurement at the positions where the probe's intensity is not too small.

C. Integration filter

Equation 1 shows that we obtain the average value of $\partial n/\partial\zeta$ if we measure the frequency change. Thus, in order to get the electron density distribution, we need to integrate the term once with respect to position in laser's frame of reference, ζ. However, if the integration is done by getting the cumulative sum of $\partial n/\partial\zeta$, a small DC offset could cause the result being tilted.

In order to suppress the DC offset error, we apply a filter to do the integration. Figure 1 shows the amplitude and phase response of our filter. For normal integral, the amplitude response at low frequency is very high. Thus in our filter, we suppress the amplitude response at the low frequency to avoid the result being tilted. We also cut the high frequency terms in our filter to avoid unwanted noise in the signal. Figure 2 shows the comparison between the integration using our filter and cumulative sum.

IV. RESULTS AND DISCUSSION

A. Measurement results

From the simulation results, we obtain the electric field of the probe pulse. Applying equation 2 produces the Wigner distribution of the signal in phase space. One example of the Wigner distribution of a signal is shown in figure 3. In the distribution, we observe the photon acceleration effect. The frequency at some positions increases and the frequency at the other positions decreases.

From the Wigner distribution of the electric field, we can get the local frequency for every position in the laser's

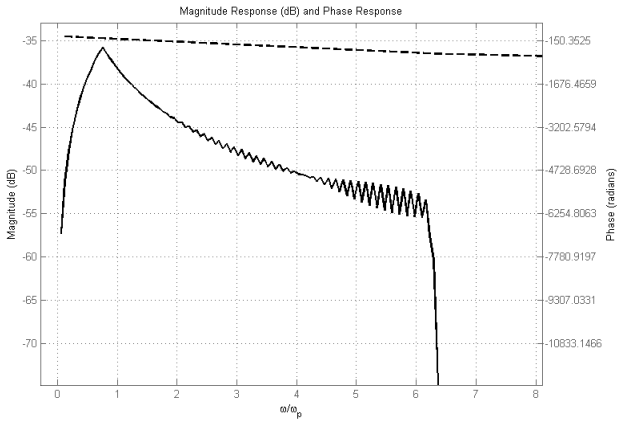

FIG. 1. Amplitude and phase response of our integration filter. Amplitude response is shown in solid line and phase response is shown in dashed line.

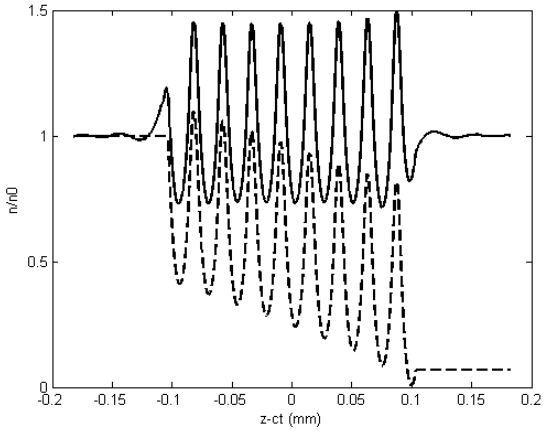

FIG. 2. Comparison of integration results using designed filter (solid line) and cumulative sum (dashed line).

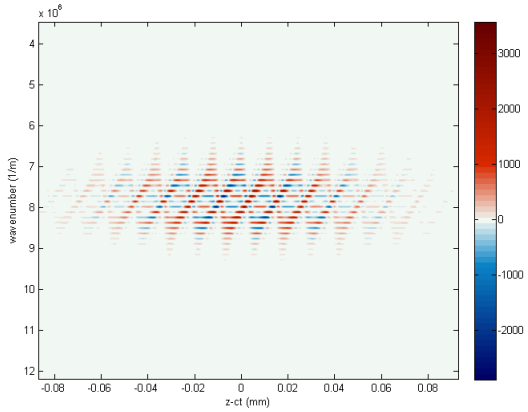

FIG. 3. (Color online) Wigner distribution of electric field of the probe after propagated 1.9mm in the plasma. Alternating values in the distribution are caused by the cross-terms.

reference frame using equation 3. By using equation 1 and the integration of $\partial n/\partial\zeta$ once, we obtain the electron density profile of the plasma.

According to equation 3, accuracy of the measurement would be good if the intensity at that point is not very small or not too far from the probe's centre. Because of that, we did the measurements only at positions where the intensity is more than 0.5% of the maximum intensity. At the other positions, we take the frequency change as zero to avoid large inaccuracy. The lower we choose the threshold value, the wider measurement result we can obtain, but the inaccuracy also increases.

Figure 4 shows the comparison between the measured electron density and the actual density over the distance. At $z-ct < 0.1$ mm, we see some noise in the actual values. The noise is caused by the probe's electric field. Over the propagation distance less than 6 mm, the measurement agrees well with the actual average value. However, if the laser pulse propagates too far, the measurement fails to match with the actual value. This is because of photon trapping effect, which we will explain in section IV B 2.

In order to determine the accuracy of the measurement, we provide the normalised root mean square error (NRMSE) between measurement and actual values. The NRMSE is defined by

$$NRMSE = \frac{RMSE}{\max(n_a) - \min(n_a)}$$
$$RMSE = \sqrt{\frac{1}{\zeta_0}\int \left[n_m(\zeta) - n_a(\zeta)\right]^2 d\zeta} \qquad (4)$$

where ζ_0 denotes the range in position where the NRMSE would be calculated, $n_m(\zeta)$ and $n_a(\zeta)$ respectively denote the measured and the actual values as function of position in the laser's reference frame, ζ. Before calculating the NRMSE values, we remove the noise at $z - ct < 0.1$ mm from actual density values by applying a low pass filter.

The NRMSE of the measurement is shown in figure 5 for several propagation distance. As shown in the graph, the measurement achieves less than 10% NRMSE over the propagation distance less than 6 mm. After propagates 6 mm, the error increases and becomes unstable. This is where the photon trapping effect occurs.

B. Measurement constraints

In doing measurements using the photon acceleration technique, there are several constraints and limitations that we need to take into account. In this paper, we discuss three constraints and limitations: the small frequency change, photon trapping, and displacement of the laser.

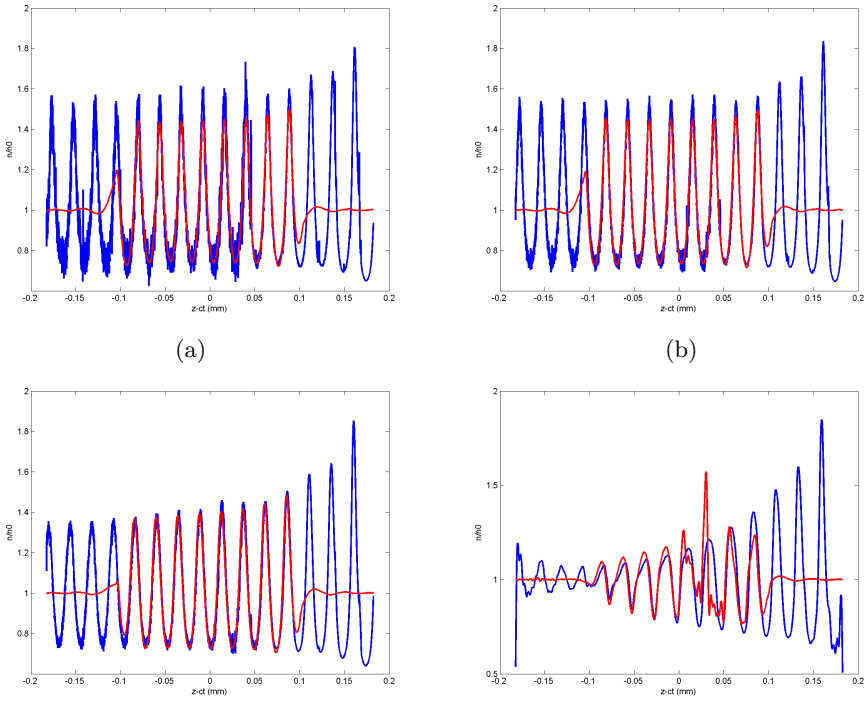

FIG. 4. (Color online) Comparison of measured longitudinal electric field (red line) and the actual longitudinal electric field averaged over the distance (blue line) when the laser has propagated (a) 0.8 mm, (b) 1.9 mm, (c) 3.8 mm, and (d) 6.3 mm. The measurement only takes place from about −0.1 mm to 0.1 mm relative to the centre of the pulse.

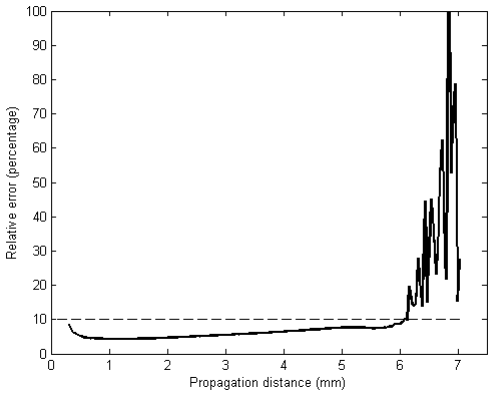

FIG. 5. Normalised root mean square error (NRMSE) between measured and actual values from the simulation, shown in percentage. The NRMSE values were calculated from the position −50 μm to 50 μm relative to the probe's centre.

1. *Small frequency change*

The first limitation is when the frequency change is not observable. The frequency change in photon acceleration in some cases is very small and thus very hard to measure precisely. As an example, for the AWAKE experiment [29], the frequency change would be $\sim 3\%$. Thus we need an equipment with precision up to $\sim 0.03\%$ to make a good measurement.

Moreover, a short pulse can have a broad frequency spectrum. If the pulse is too short and the frequency change is too small, it would be also too hard to observe the frequency change. In order to make the measurement easier, the laser's frequency change should be greater than bandwidth of the pulse or $\Delta\omega > \omega_{bw}$. By considering the Gabor limit [30], $\tau_{pulse}(\omega_{bw}/2\pi) \geq 1/2$, and equation 1, the minimum duration of the probe pulse should be

$$\tau_{pulse} > \frac{2\pi\omega_0 n_0}{\omega_p^2 s}\left(\frac{\partial n}{\partial \zeta}\right)^{-1}, \tag{5}$$

where ω_0 is the central frequency of the pulse, n_0 is the density of the plasma, ω_p is frequency of the plasma wakefield, s is the propagation distance, and $\partial n/\partial\zeta$ is partial derivative of electron density to the position in the laser's frame of reference.

In this case, the minimum pulse duration is about 3 fs, much smaller than the plasma wavelength which is around 80 fs. Therefore this limitation is not significant in this case. However, this limitation should be considered when doing measurement at low density plasma.

2. Photon trapping

In photon acceleration, the frequency of some photons increase and some decrease. Based on the plasma dispersion relation, $\omega^2 = \omega_p^2 + k^2c^2$, the photons whose frequency increases will acquire higher group velocity and the others will acquire lower group velocity. The difference of this group velocity causes some photons to be gathered in the troughs and be away from the peaks of the wakefield. This mechanism is called photon trapping [20], which is one form of modulation instabilities [26–28].

Photon trapping could cause trouble in doing measurements with photon acceleration technique. As the intensity of the laser at some points approaches zero, the error in obtaining the frequency will be very high and could cause high inaccuracy.

The photon trapping mechanism starts when the laser enters the plasma. However, this effect is negligible at the beginning and would become significant after propagating some distance. We can estimate the propagation distance scale length in which the photon trapping would be significant. The propagation distance scale length is approximately

$$s_{trap} \approx \lambda_p \left(\frac{\omega_0}{\omega_p}\right)^2 \left(\frac{\delta n}{n_0}\right)^{-0.5}, \tag{6}$$

where λ_p is the plasma wavelength and $\delta n/n_0$ is the relative perturbation of the wakefield.

For the laser and plasma parameters considered here, the propagation distance scale length of photon trapping is about ~ 30 mm. And from figure 5, we observe the photon trapping effect at 6 mm. Therefore, the photon trapping effect should be considered after propagated 20% of s_{trap} in this case.

One way to determine if the photon trapping should be taken into account is by looking at the intensity distribution of the laser obtained by equation 3. Figure 6 shows the laser's intensity distribution at several propagation distances. As shown in the figures, the laser intensity gets modulated as it travels along the plasma. And at some distance, the laser intensity at some points go to zero and intensity at some points become very high as shown on figure 6d. This shows that the photon trapping has occurred.

3. Laser displacement

Up to this point, we assumed that the laser is always moving along with the wakefield. However, this may not be true for all cases. If the group velocity of the probe pulse is not same as the phase velocity of the wakefield, the laser could be displaced with respect to the wakefield.

In this case, the pump pulse and the probe pulse have the same frequency, thus the group velocity of the probe pulse and phase velocity of the wakefield should be the same. However, in some cases it is very hard to get the right frequency of probe pulse to get the same velocity. In those cases, the laser displacement should be considered because it changes the measurement values.

To show the effect of laser displacement, we performed a simulation with the same conditions but with a probe wavelength of 1600 nm. Figure 7 shows the measurement result using this probe compared with the actual average density after it travels 1.4 mm. As shown in the figure, the measurement result is shifted backward by 1.6 μm and slightly smaller than the actual value. This shift is caused by the difference of group velocity of the probe pulse and phase velocity of the wakefield.

Using equation 1 and by considering that the pulse is moving relative to the wakefield, we obtain a total shift of the measurement as,

$$\Delta s \approx \frac{s}{2v_p}(v_g - v_p), \tag{7}$$

where v_g and v_p are group velocity of the laser probe pulse and phase velocity of the plasma, respectively, and s is the propagation distance. Equation 7 also assumes that the wakefield amplitude is constant and not changing over the time. For the case with probe wavelength of 1600 nm, equation 7 gives $\Delta s = -1.2$ μm with $s = 1.4$ mm, while the simulation result gives -1.6 μm.

Besides the horizontal shifting, the laser displacement effect also caused the measurement values to be scaled down slightly. By doing the same derivation with equation 7, we can get the decrement of the measured values because of laser displacement as below,

$$\frac{\Delta n}{n - n_0} \approx -\frac{1}{24}k_p^2 s^2 (v_g - v_p)^2/c^2. \tag{8}$$

Thus, if the laser propagates for long distance, the correction above should be taken into account to increase the measurement accuracy.

V. CONCLUSIONS

Results from our simulation show that the measurement of a density profile in a plasma wakefield can be performed using photon acceleration. The measurement is done by sending a long laser probe pulse behind the short pump pulse which generates the wakefield. From our simulation results, the measurement values achieve a normalised root mean square error of less than 10%, although the exact region needs to be determined for a given set of experimental parameters.

There are also limitations and constraints to be considered before doing a photon acceleration measurement. Those are small frequency changes, photon trapping effects, and laser displacement. If the propagation distance is too small, then the frequency change could be undetectable. However, if the propagation distance is too far, the photon trapping effect could spoil the measurement result. Also, if the probe's group velocity is not same

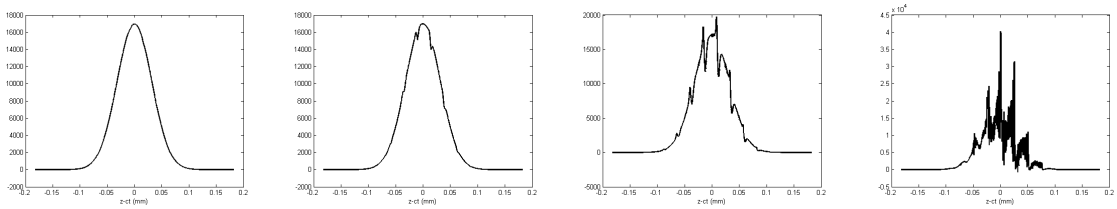

(a) (b) (c) (d)

FIG. 6. Distribution of the laser intensity when the laser has propagated (a) 0.8 mm, (b) 1.9 mm, (c) 3.8 mm, and (d) 6.3 mm. The measurement only takes place from about −0.1 mm to 0.1 mm relative to the centre of the pulse. The last picture shows that the photon trapping occurs and causes intensity at some points go to zero.

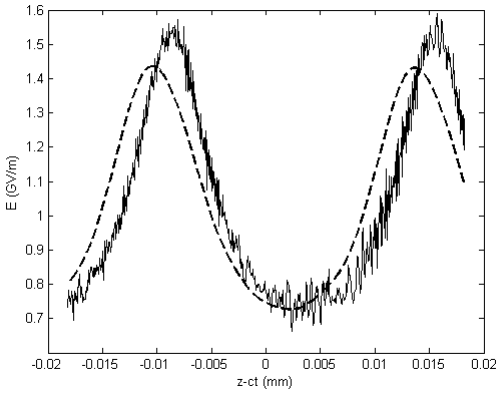

FIG. 7. Measurement result of longitudinal average electric field with probe wavelength of 1600 nm after travelling 1.4 mm. The measurement result (dashed line) is shifted backward by 1.6 μm relative to the actual value (solid line).

with the phase velocity of the wakefield, the inaccuracy of the measurement could also increase. By considering these effects, we can determine the optimal frequency of the probe and propagation distance for a given set of experimental parameters.

ACKNOWLEDGMENTS

The authors would like to acknowledge the support from Computer Science Department at the Rutherford Appleton Laboratory for the use of SCARF-LEXICON computer cluster. We also wish to thank the OSIRIS consortium for the use of OSIRIS and also to Science and Technology Facilities Council for its support to UK-AWAKE. One of the authors (M. F. Kasim) would like to thank Indonesian Endowment Fund for Education for its support. M. Wing acknowledges the support of DESY, Hamburg. The work is part of EuCARD-2, partly funded by the European Commission, GA 312453.

[1] J. Faure, Y. Glinec, A. Pukhov, S. Kiselev, S. Gordienko, E. Lefebvre, J.-P. Rousseau, F. Burgy, and V. Malka, Nature **431**, 541 (2004).

[2] W. P. Leemans, B. Nagler, A. J. Gonsalves, Cs. Tth, K. Nakamura, C. G. R. Geddes, E. Esarey, C. B. Schroeder, and S. M. Hooker, Nature Phys. **2**, 696 (2006).

[3] S. P. D. Mangles, C. D. Murphy, Z. Najmudin, A. G. R. Thomas, J. L. Collier, A. E. Dangor, *et al.*, Nature **431**, 535 (2004).

[4] C. G. R. Geddes, Cs. Toth, J. van Tilborg, E. Esarey, C. B. Schroeder, D. Bruhwiler, C. Nieter, J. Cary, and W. P. Leemans, Nature **431**, 538 (2004).

[5] T. Tajima and J. M. Dawson, Phys. Rev. Lett. **43**, 267 (1979).

[6] C. Joshi, W. B. Mori, T. Katsouleas, J. M. Dawson, J. M. Kindel, and D. W. Forslund, Nature **311**, 525 (1984).

[7] J. B. Rosenzweig, D. B. Cline, B. Cole, H. Figueroa, W. Gai, R. Konecny, J. Norem, P. Schoessow, and J. Simpson, Phys. Rev. Lett. **61**, 98 (1988).

[8] A. Caldwell, K. Lotov, A. Pukhov, and F. Simon, Nature Phys. **5**, 363 (2009).

[9] E. Esarey, C. B. Schroeder, and W. P. Leemans, Rev. Mod. Phys. **81**, 1229 (2009).

[10] D. Gordon, K. C. Tzeng, C. E. Clayton, A. E. Dangor, V. Malka, K. A. Marsh, A. Modena, W. B. Mori, P. Muggli, Z. Najmudin, D. Neely, C. Danson, and C. Joshi, Phys. Rev. Lett. **80**, 2133 (1998).

[11] V. Malka, S. Fritzler, E. Lefebvre, M.-M. Aleonard, F. Burgy, J.-P. Chambaret, J.-F. Chemin, K. Krushelnick, G. Malka, S. P. D. Mangles, Z. Najmudin, *et al.*, Science **298**, 1596 (2002).

[12] C. W. Siders, S. P. Le Blanc, A. Babine, A. Stepanov, A. Sergeev, T. Tajima, and M. C. Downer, IEEE Trans. Plasma Sci. **24**, 301 (1996).

[13] S. P. Le Blanc, E. W. Gaul, N. H. Matlis, A. Rundquist, and M. C. Downer, Opt. Lett. **25**, 764 (2000).

[14] N. H. Matlis, S. Reed, S. S. Bulanov, V. Chvykov, G. Kalintchenko, T. Matsuoka, P. Rousseau, V. Yanovsky, A. Maximchuk, S. Kalmykov, G. Shvets, and M. C. Downer, Nature Phys. **2** 749 (2006).

[15] A. Maksimchuk, S. Reed, S. S. Bulanov, V. Chvykov, G. Kalintchenko, T. Matsuoka, C. McGuffey, G. Mourou, N. Naumova, J. Nees, P. Rousseau, *et al.*, Phys. Plasmas **15**, 056703 (2008).

[16] A. Svert, S. P. D. Mangles, M. Schnell, J. M. Cole, M. Nicolai, M. Reuter, M. B. Schwab, M. Mller, K. Poder,

O. Jckel, G. G. Paulus, C. Spielmann, Z. Najmudin, M. C. Kaluza, arXiv:1402.3052 (2014).
[17] J. M. Dias, L. O. Silva, and J. T. Mendonça, Phys. Rev. ST Accel. Beams **1**, 031301 (1999).
[18] C. D. Murphy, R. Trines, J. Vieira, A. J. W. Reitsma, R. Bingham, J. L. Collier, E. J. Divall, P. S. Foster, C. J. Hooker, A. J. Langley, P. A. Norreys, *et al.*, Phys. Plasmas **13**, 033108 (2006).
[19] R. M. G. M. Trines, C. D. Murphy, K. L. Lancaster, O. Chekhlov, P. A. Norreys, R. Bingham, J. T. Mendonça, L. O. Silva, *et al.*, Plasma Phys. Control. Fusion **51**, 024008 (2004).
[20] J. T. Mendonça, *Theory of Photon Acceleration* (CRC Press, 2001).
[21] J. Schreiber, C. Bellei, S. P. D. Mangles, C. Kamperidis, S. Kneip, S. R. Nagel, C. A. J. Palmer, P. P. Rajeev, and Z. Najmudin, Phys. Rev. Lett. **105**, 235003 (2010).
[22] R. A. Fonseca, *et al.*, Lecture Notes in Computer Science Vol. 2329, III-342 (Springer, Heidelberg, 2002).
[23] C. K. Birdsall and A. B. Langdon, *Plasma Physics via Computer Simulation* (CRC Press, 2004).
[24] E. Wigner, Phys. Rev. **40**, 749 (1932).
[25] P. Flandrin, *Time-Frequency/Time-Scale Analysis* (Academic Press, 1999).
[26] F. F. Chen, *Introduction to Plasma Physics and Controlled Fusion* vol 1 (Springer, 2006).
[27] K. Nishikawa, *Advances in Plasma Physics* vol 6 ed A. Simon and W. B. Thomson (New York: Wiley, 1976).
[28] R. Bingham and C. N. Lashmore-Davies, Plasma Phys. Control. Fusion **21**, 433 (1979).
[29] A. Caldwell, E. Gschwendtner, K. Lotov, P. Muggli, M. Wing, *et al.*, CERN-SPSC-2013-013, http://cds.cern.ch/record/1537318, and arXiv:1401.4823 (2013).
[30] D. Gabor, Journal of the Institution of Electrical Engineers-Part III: Radio and Communication Engineering, Vol. 93 Issue 26 (1946) p. 429-441.